The paradox of adaptive trait clines with nonclinal patterns in the underlying genes

Katie E. Lotterhos[a,1] iD

Multivariate climate change presents an urgent need to understand how species adapt to complex environments. Population genetic theory predicts that loci under selection will form monotonic allele frequency clines with their selective environment, which has led to the wide use of genotype–environment associations (GEAs). This study used a set of simulations to elucidate the conditions under which allele frequency clines are more or less likely to evolve as multiple quantitative traits adapt to multivariate environments. Phenotypic clines evolved with nonmonotonic (i.e., nonclinal) patterns in allele frequencies under conditions that promoted unique combinations of mutations to achieve the multivariate optimum in different parts of the landscape. Such conditions resulted from interactions among landscape, demography, pleiotropy, and genetic architecture. GEA methods failed to accurately infer the genetic basis of adaptation under a range of scenarios due to first principles (clinal patterns did not evolve) or statistical issues (clinal patterns evolved but were not detected due to overcorrection for structure). Despite the limitations of GEAs, this study shows that a back-transformation of multivariate ordination can accurately predict individual multivariate traits from genotype and environmental data regardless of whether inference from GEAs was accurate. In addition, frameworks are introduced that can be used by empiricists to quantify the importance of clinal alleles in adaptation. This research highlights that multivariate trait prediction from genotype and environmental data can lead to accurate inference regardless of whether the underlying loci display clinal or nonmonotonic patterns.

genome-wide associations | multivariate ordination | local adaptation | pleiotropy | polygenic

Clines have a rich history of study in biology. Clines are a monotonic gradient in a measurable character, genotype, or allele frequency (modified from ref. 1). Starting around the 1950s, population geneticists became interested in selection in continuous populations along environmental gradients (2–4). Population genetic theory developed then for a single locus under a gradient of selection predicted that clines in allele frequency will evolve (2, 5–8). Even multilocus models of polygenic adaptation across an environmental gradient predict that phenotypic clines will evolve by a series of staggered allele frequency clines (9–11).

As a result of this theory, ecological geneticists have long searched for clinal patterns in allele frequencies, dating back to *Drosophila* chromosome inversions (12) and many studies in allozymes (13). Now, the search for allele frequency clines has extended to the genome, to uncover the genetic basis of adaptation to the environment (13–15). Verbal arguments have claimed that beneficial variants with weak phenotypic effects will lead to "subtle shifts" in allele frequency that correlate with environmental variables (16–18), or a subtle cline. Statistical approaches known as "genotype–environment associations" [genotype–environment associations (GEAs), sensu 19] have been developed to determine if a cline between an allele frequency and an environmental gradient is significant after correction for neutral population structure.

GEA methods are based on the concept that adaptive alleles will form clines with a selective environment. Since 2010, the most widely used methods (20–25), reviews (11, 14, 15, 26), methods evaluations (27–32), and high-profile applications of GEA methods in different taxa (18, 33–37) have been cited over 7,700 times (Google Scholar, July 2022). A scientific paradigm is a distinct set of concepts, thought patterns, research methods, and standards for what constitutes legitimate contributions to a field. The GEA concept meets this definition, and more specifically Kuhn's "local" paradigm (i.e., a typical example) for how to study the genetic basis of adaptation to the environment (38, 39). Although other tests such as outlier tests for genetic differentiation exist, these tests do not explicitly link genetic differences to the environment (15).

GEA methods have been largely tested against data simulated under the assumption that the fitness of one allele increases along an environmental gradient while the other decreases, which evolves allele frequency associations with the climate variable (14, 20, 22–24, 27–30).

Significance

Population geneticists have historically modeled adaptation in meta-populations to a single environmental gradient, which evolves monotonic clinal patterns in allele frequency at the loci under selection. This study shows that under complex multivariate adaptation, trait clines can evolve despite nonmonotonic allele frequency patterns across environmental gradients. These patterns are not discovered by genotype–environment association methods, which are widely used to discover adaptation. This result challenges widely held conceptual models of adaptation via subtle shifts in allele frequencies across environmental gradients and can explain why genes that underlie environmental traits do not always evolve clines. Additionally, this study shows that even when inference from genotype–environment association methods is inaccurate, multivariate quantitative traits can still be accurately estimated from genotypes and environments.

Author affiliations: ªDepartment of Marine and Environmental Sciences, Northeastern University Marine Science Center, Nahant, MA 01908

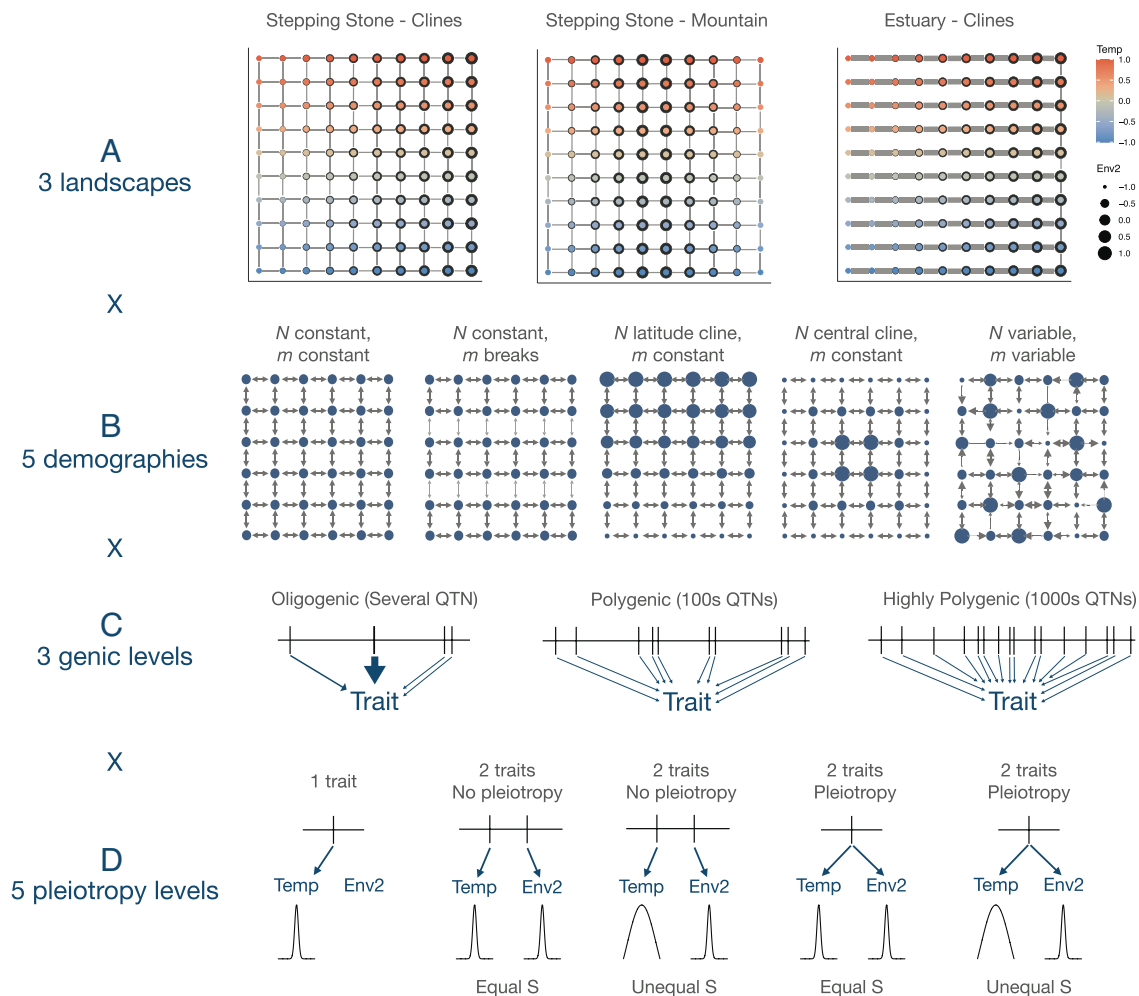[1]Email: k.lotterhos@northeastern.edu.

Fig. 1. An overview of the parameter levels for the simulations with two quantitative traits. (*A*) Three landscapes determined the relationship between patterns of migration and the selective environment. The color of the point indicates the optimum multivariate trait value at that location on the landscape. The optimum temperature (*Temp*) trait followed a latitudinal cline in all landscapes, while the optimum *Env2* depended on the landscape. Gray lines indicate pathways of migration, and their thickness represents the migration rate. (*B*) Five demographies determined how drift and migration operated across the landscape (examples shown for stepping stone). (*C*) Three genic levels determined the number of loci (vertical dashes) and their effect sizes (arrow thickness) on the trait. (*D*) Five pleiotropy levels determined the number of traits, pleiotropic effects of mutations, and strength of selection on each trait.

This practice may have led to overly optimistic performance of GEAs for two reasons. First, what if the evolution of local adaptation does not evolve clines in frequency at the selected alleles (the first principles issue)? Second, even when allelic clines do evolve, GEAs may undercorrect or overcorrect for structure, leading to a failure to accurately detect the loci under selection (the statistical issue). Another statistical issue is whether the accuracy of multivariate ordination (to infer multivariate adaptation to multiple environments) is affected by a lack of clinal patterns in the data. If these issues prove to be relevant, then reliance on the study of clines will hinder detection of the genetic basis of adaptation and translation of genomic data to species conservation.

The goals of this study were to i) understand the conditions under which allele frequency clines are more or less likely to evolve as quantitative traits adapt to complex environments, ii) study the ability of univariate [correlation, latent factor mixed models] and multivariate (redundancy analysis) GEA methods to correctly infer the genetic basis of adaptation, and iii) show that, even when the genetic architecture could not be accurately inferred by GEAs, multivariate quantitative traits can be estimated from genotype and environmental data through a back-transformation of ordination space. To achieve these goals, an innovative set of simulations were developed that included i) up to two quantitative traits, each

adapting to a different environmental pattern, ii) genetic architectures ranging from oligogenic (a few loci with large effects on the trait) to highly polygenic (thousands of loci with small effects), iii) pleiotropic or nonpleiotropic mutational effects, and iv) complex landscapes and demographies (Fig. 1). Alleles had additive effects on the quantitative traits, which were under stabilizing selection within populations but the optimum trait value was linearly associated with the selective environment. Across all simulations, clines evolved between the quantitative trait and its selective environment, but with varying proportions of quantitative trait nucleotides (QTNs) that evolved clines.

Results

I conducted replicate forward-time simulations of a metapopulation adapting to a heterogeneous spatial environment with SLiM v. 3.6 (40, 41) to create single-nucleotide polymorphism data for each individual. I simulated 225 parameter levels (15 demographies × 15 genetic architectures) of 10 replicates each, for a total of 2,250 simulations. The levels varied in i) the relationship between the landscape and the environmental trait optimum (in Stepping Stone Clines and Estuary Clines geographic distance corresponded to environmental distance; in Stepping Stone Mountain it did not

Fig. 1A), ii) the demography described by migration rates and effective population size (with cases that confounded genetic drift with selection and cases that confounded population structure with selection, Fig. 1B), iii) the genic level of both traits (with cases spanning from oligogenic to highly polygenic, Fig. 1C), and iv) the pleiotropic effects of mutations on traits (with cases spanning from one trait, to two traits with and without pleiotropy, and with different strengths in selection on each trait, Fig. 1D). Thus, the simulations spanned scenarios from those that are commonly simulated in the population genetics literature (one oligogenic trait adapting to an environmental cline) to previously unexplored scenarios (two polygenic traits with pleiotropy).

The two traits included a "temperature" trait that adapted to a latitudinal environment (in all simulations), and an "Env2" trait that adapted to a longitudinal environment (only in 2-trait simulations). The biological analogy to *Env2* depended on the context: it is analogous to elevation in the Stepping Stone Mountain landscape (e.g., trees) or salinity in the Estuary Clines landscape (e.g., sticklebacks or oysters) (Fig. 1A).

The simulations reached an equilibrium level of local adaptation (*SI Appendix*, Fig. S1), and the amount of divergence was primarily determined by landscape and demography, while the degree of local adaptation (LA) was primarily determined by selection strength (*SI Appendix*, Figs. S1–S4 and Tables S1 and S2). Population structure (measured as PC1 of the genotype matrix) was highly correlated with deme temperature in all simulations, but rarely correlated with *Env2* in the Stepping-Stone-Mountain or Estuary-Clines landscapes (*SI Appendix*, Fig. S5). Oligogenic, moderately polygenic, and highly polygenic architectures evolved on average 12, 646, and 3,042 QTNs, but this was reduced to 8, 58, and 499, respectively, after filtering for minor allele frequency (MAF) (*SI Appendix*, Fig. S6). Additional information about the simulations can be found in *SI Appendix, Supplemental Results*.

Evolutionary Processes That Affect the Proportion of Clinal QTNs. Across all simulations, trait clines between each quantitative trait and the selective environment evolved (with correlations typically between 0.55 and 0.9, *x* axis in Fig. 2A). Hereafter, "clinal QTNs" are those with significant associations between allele frequency and an environmental variable after correction for multiple tests. Despite high correlations evolving between environmental traits and deme environments across all simulations, the percent of clinal QTNs ranged from 0 to 100% (*y* axis in Fig. 2A). Therefore, the simulations are useful for understanding how trait clines can evolve with or without GEA patterns at the underlying loci.

Interactions among landscape, demography, and genetic architecture determine the proportion of QTNs with clinal patterns. The simulations that evolved a large proportion of clinal QTNs were simulations with oligogenic architectures and no pleiotropy (Fig. 2 A and B). The proportion of clinal QTNs decreased as the genetic architecture became more polygenic (Fig. 2B). There was an interaction between genic level and pleiotropy, as pleiotropy reduced the proportion of clinal QTNs by ~40% in oligogenic architectures, but this effect became less pronounced as the architecture became more polygenic (Fig. 2B, compare bars within genic level). In addition, the proportion of clinal QTNs decreased as the strength of selection became weaker, but was not substantially affected by demography (*SI Appendix*, Fig. S7).

When only the temperature trait was simulated alone, a similar proportion of temperature QTNs evolved clines across all landscapes (Fig. 2C, compare medians within "one Trait"), which is consistent with the relationship between the temperature trait optimum and spatial location being the same among the landscapes (Fig. 1A). However, when the temperature trait was simulated in conjunction with the *Env2* trait, a slightly decreased proportion of temperature QTNs evolved clines (Fig. 2C, compare medians for one Trait vs. "two Traits" in the same color bar).

The landscape greatly affected the proportion of *Env2* QTNs that evolved clines. In the Stepping-Stone-Clines landscape, the proportion of *Env2* QTNs that evolved clines was similar to the proportion of temperature QTNs that evolved clines (compare dark purple bar in Fig. 2D with Fig. 2C, two traits), which is consistent with this landscape being symmetrical with regard to gene flow in both environments. However, the proportion of *Env2* QTNs with clines decreased in the Stepping-Stone-Mountain scenario and was greatly reduced in the Estuary-Clines scenario (Fig. 2D).

Trait clines evolved with nonclinal patterns in the underlying allele frequencies under conditions that promoted unique combinations of mutations to evolve to the multivariate optimum in different parts of the landscape. Consider an example from the Estuary demography with a pleiotropic and moderately polygenic architecture: Phenotypic clines evolved in both traits, but with more variance for the *Env2* trait that experienced higher gene flow (Fig. 3 A and B). Many temperature QTNs exhibited nonmonotonic relationships between allele frequency and deme temperature (Fig. 3C), while most *Env2* QTNs showed no apparent pattern (Fig. 3D). These patterns were caused by unique sets of alleles that evolved in response to the unique multivariate optima at each inner estuary site (Fig. 3 E and F); a phenomenon that was exacerbated by lack of gene flow between the inner estuary sites. The same phenomenon was observed in the Stepping-Stone-Mountain simulations, except in this case unique genetic architectures evolved to the same multivariate optimum in the upper corners or lower corners of the landscape (e.g., convergent evolution for the trait), because of lack of gene flow between these locations (42).

As architectures became more polygenic, a larger number of genetic routes were available to achieve the same trait value (e.g., high genotypic redundancy, sensu 43). This led to more unique sets of alleles evolving to the multivariate optima in each deme, and hence fewer allele frequency clines. Genotypic redundancy, however, was not a prerequisite for lack of clines at QTNs. Under oligogenic architectures with low genotypic redundancy, pleiotropy led to fewer clines at QTNs (Fig. 2B) because a pleiotropic mutation in a single patch could bring that deme closer to the multivariate optimum in that patch: Pleiotropy promoted unique combinations of mutations to evolve to the multivariate optimum in different demes, which reduced GEA patterns.

Note that due to the arbitrary choice of simulation parameters, the proportion of simulations that evolved clines does not reflect the frequency that clines are expected to evolve in nature. The simulations are only useful for understanding the conditions that trait clines evolve with or without GEA patterns at the underlying QTNs.

To What Extent Do GEAs Accurately Infer the Genetic Basis of Adaptation? Each simulation was analyzed with GEA methods commonly used to identify clinal alleles as outliers beyond that expected by neutrality: Kendall's τ rank correlation between genotype and environment (no structure correction), latent factor mixed model [LFMM, univariate, includes structure correction (20, 21, 25)] and redundancy analysis [RDA, multivariate ordination, with and without structure correction (29, 31, 32, 44)].

While structure correction greatly reduced false discovery rates for the univariate models, the multivariate RDA showed high false discovery rates with and without structure correction (Fig. 4A and *SI Appendix*, Fig. S8). Power to detect QTNs was generally less than 60% across all approaches, and power was reduced by ~30 to
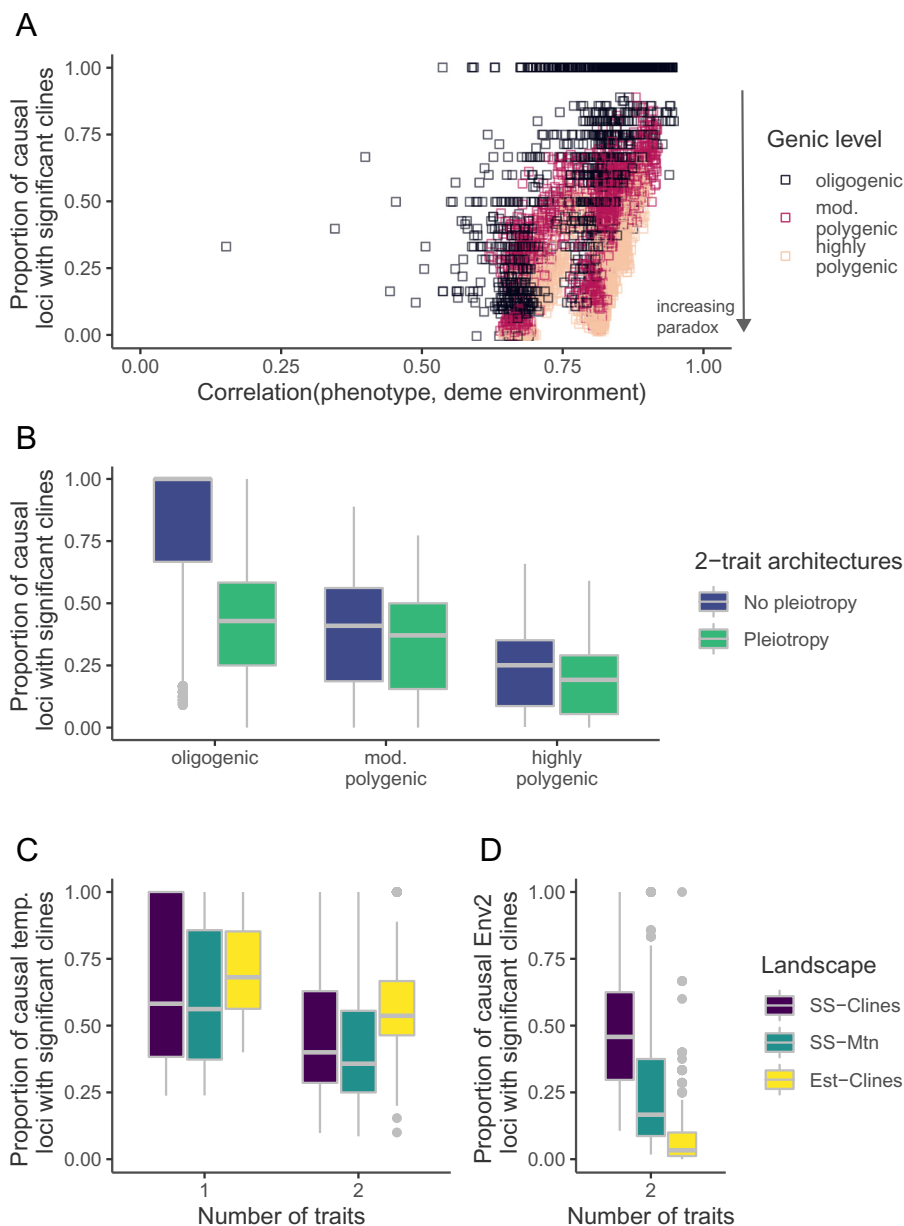
Fig. 2. Effect of different parameter levels on the proportion of quantitative trait nucleotide (QTN) loci that evolved significant clines. (*A*) Scatterplot of the proportion of causal QTN loci that have significant allele frequency clines as a function of the degree of the evolved cline in the trait under selection. (*B*) The effect of genic level and pleiotropy level, averaged over both traits. (*C*) The proportion of temperature QTNs that evolved significant clines with the temperature environment, split out by landscape (color) or by whether the trait was simulated alone or in combination with a second trait (Number of traits). (*D*) The effect of the landscape on the proportion of *Env2* QTNs that evolved significant clines with the *Env2* environment (which was only simulated in combination with the temperature trait). Abbreviations: *SS-Clines*: stepping stone landscape with clines in both environments; *SS-Mtn*: stepping stone landscape with clines in temperature environment but mountain range for *Env2*; *Est-Clines*: estuary landscape with clines in both environments. See Fig. 1 for landscapes.

50% after structure correction for the temperature model (Fig. 4*B*). This occurred because structure correction caused power to decline as the correlation between structure and environment increased (especially at a correlation > 0.25, Fig. 4*C* and *SI Appendix,* Fig. S9), and temperature was highly correlated with structure across all simulations (*SI Appendix,* Fig. S5). Thus, in traits that evolved the highest proportion of clinal QTNs, GEA outlier approaches could have the least accurate inference due to structure correction.

Frameworks to Determine How Important Clinal QTNs Are in Adaptation. The observation of nonclinal patterns in QTNs raise questions about the importance of clinal QTNs in adaptation. Here I introduce three different frameworks that could be applied to empirical data to quantitatively answer this question.

The first framework quantifies the proportion of candidate loci from a genome-wide association study (GWAS) or quantitative-trait locus (QTL) mapping study that shows clinal relationships with an environmental variable ($\hat{p}_{\text{GWAS}}$). A requirement for this framework is that the trait chosen for the GWAS shows a clinal relationship with the environmental variable. In the simulations, the accuracy of this framework depended on the underlying genetic architecture (*SI Appendix,* Fig. S10). When the underlying genetic architecture was highly polygenic, $\hat{p}_{\text{GWAS}}$ scaled directly with the known proportion of QTNs that were clinal. As the architecture became more oligogenic, $\hat{p}_{\text{GWAS}}$ became an underestimate of the proportion of QTNs that were clinal due to a lower ratio of true positives to false positives in the candidate hits.
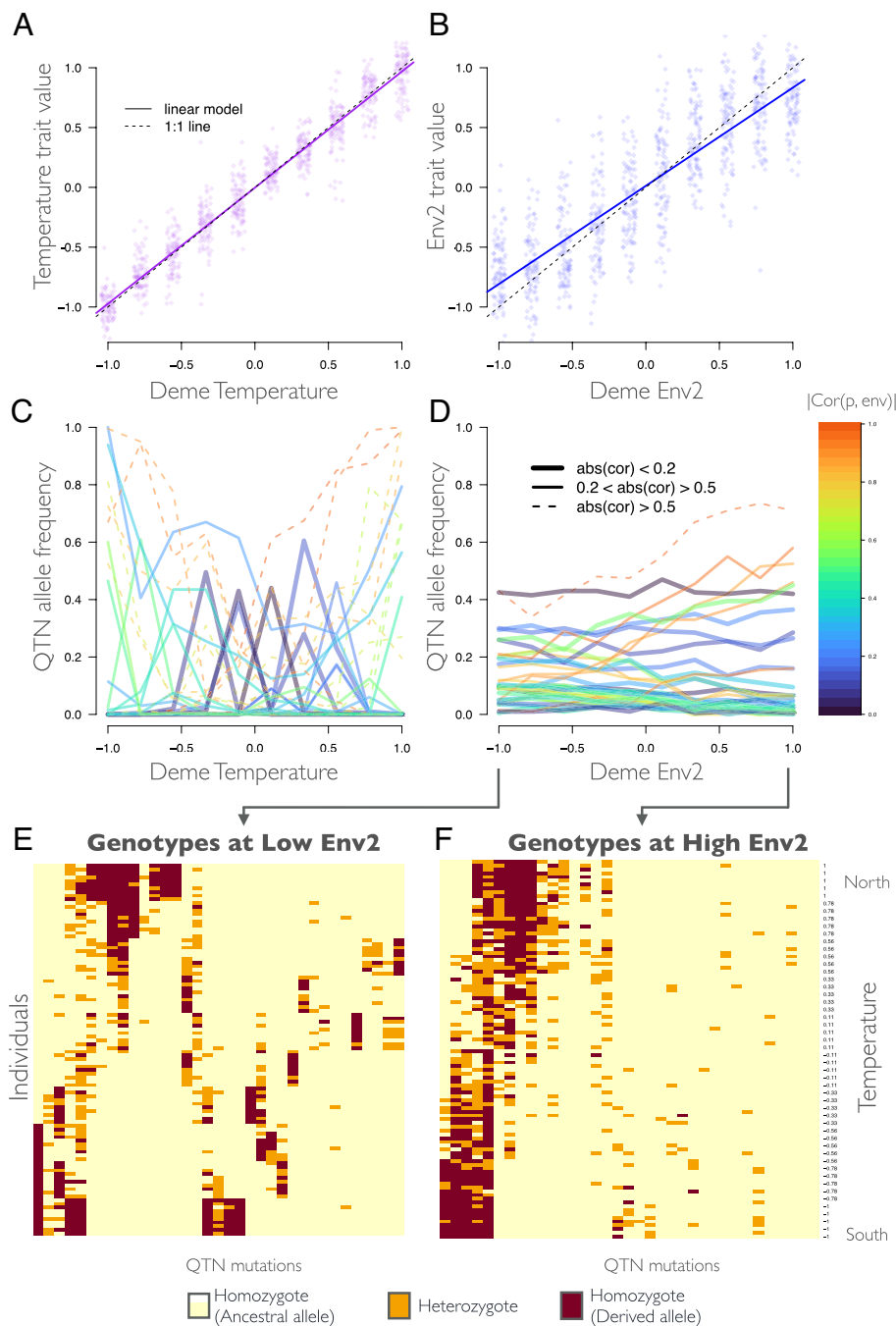
Fig. 3. Evolution of phenotypic clines with nonclinal patterns in allele frequencies from an Estuary-clines simulation. (*A* and *B*) The evolved individual trait value (i.e., the sum of QTN effect sizes) as a function of deme environment for (*A*) temperature and (*B*) *Env2*. (*C* and *D*) Frequency of the derived allele at each QTN vs. deme environment for (*C*) temperature and (*D*) *Env2*. Lines types and colors indicate the strength of the absolute value of the correlation between the derived allele frequency (*p*) and the environment ($|Cor(p, env)|$). (*E* and *F*) Genotype heatmaps for individuals (in rows) at QTNs (in columns) sampled at all (*E*) low values of *Env2* or (*F*) high values of *Env2* sites. Individuals ordered from those sampled in the north (high temperatures) to the south (low temperatures). The blocks of derived alleles in *E* shows how specific mutations arose within each inner estuary site that brought the deme closer to the multivariate optimum. Parameter levels: Estuary clines landscape, moderately polygenic, two traits with pleiotropy and equal selection strength, *N* central cline, *m* constant, seed 1231214. All QTNs with minor allele frequency > 0.01 in the metapopulation sample are plotted in *C–F*.

The second framework quantifies the proportion of additive genetic variance (V_A) in the environmental trait explained by clinal QTNs ($\hat{p}_{VA}$). This framework could be applied to empirical data by approximating the V_A of i clinal alleles using their allele frequencies (p_i) and effect size estimates (α_i) from a GWAS with the environmental trait as $\Sigma\alpha_i^2 p_i(1-p_i)$, then dividing the sum by an estimate of V_A in the trait using standard quantitative genetic methods (45). In the simulations, $\hat{p}_{VA}$ could be as low as 1% or as high at 100%. With the simulations, I additionally evaluated whether the proportion of V_A explained by nonclinal QTNs was

different from a null expectation based on the proportion of QTNs that were nonclinal. For the temperature trait that evolved a lot of clinal QTNs, nonclinal QTNs contributed less to V_A than expected, while for the *Env2* trait in the Estuary-Clines landscapes the contribution of nonclinal QTNs was higher than 70% and similar to the null (*SI Appendix*, Fig. S11).

The third framework quantifies the proportion of the total local adaptation that is explained by clinal alleles ($\hat{p}_{LA}$), and is the most comprehensive but also requires the most empirical data. The heatmaps in Fig. 2 suggest that nonclinal QTNs contribute to adaptation
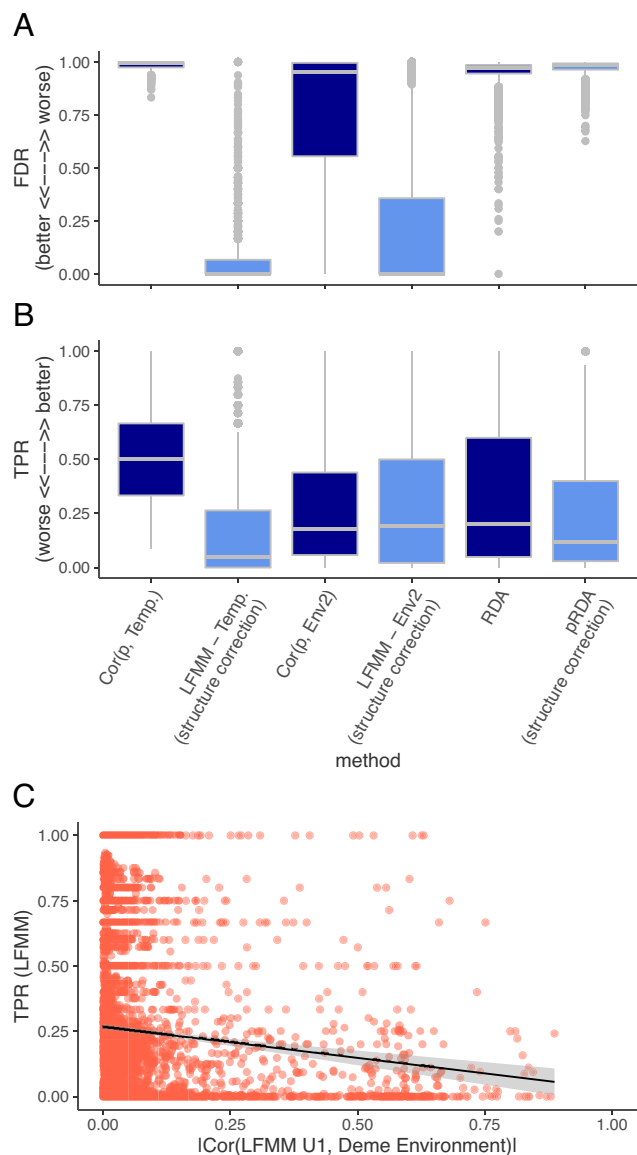
Fig. 4. Performance of different methods across all simulations. (*A*) False discovery Rate (FDR) measures the proportion of significant hits that are false positives. (*B*) True-positive rate (TPR) measures the proportion of QTN loci that are true positives. Note that the temperature environment was highly correlated with structure across all demographies, and TPR decreased more for this trait after structure correction. (*C*) Relationship between the true-positive rate of LFMM and the degree to which population structure was correlated with the environment. Population structure was approximated as the first latent factor *U1* from LFMM. Abbreviations: Cor(*p, env*): Correlation between derived allele frequency *p* and the environment; LFMM: latent factor mixed models; (p)RDA: (partial) redundancy analysis.

in specific demes, so it is possible that clinal QTNs with broadscale geographic patterns are sufficient to explain local adaptation in the metapopulation. In this framework, total local adaptation is quantified from a reciprocal transplant experiment as the mean difference in fitness between sympatry and allopatry (46), and the results of this experiment are used to quantify the functional relationship between phenotype and fitness at each site. The local adaptation explained by clinal alleles is quantified by i) calculating a breeding value for each individual from the clinal alleles in the genome and the allele effect sizes from a GWAS, ii) approximating the difference in that breeding value's fitness between sympatry and allopatry using the functional relationship between phenotype and fitness at each site, and iii) averaging that value across all individuals and dividing by the experimental total local adaptation ($\triangle_{SA}$). In the simulations, $\hat{p}_{LA}$ was generally

between 50 and 100% without structure correction (due to the higher amount of local adaptation in the *Temperature* trait that had more clinal QTNs than the *Env2* trait), but could drop below 30% after structure correction (due to overcorrection in the *Temperature* trait, which was more correlated with structure) (*SI Appendix,* Fig. S12). The effects of structure correction were nuanced and could sometimes result in an increase in the proportion of local adaptation explained by clinal QTNs because of increased power to detect *Env2* QTNs (*SI Appendix,* Figs. S12 and S13).

A Framework to Translate between Multivariate Ordination and Quantitative Genetics. RDA had high false-positive rates and low power regardless of whether structure was included in the model, indicating that it was not appropriate for the detection of QTNs. This raised the question of what multivariate ordination accurately infers about local adaptation. Interestingly, however, without structure correction individuals visually mapped onto RDA space according to their multivariate traits (e.g., Fig. 5*A*). Current interpretations of RDA loadings are limited to "population/ genotype X is correlated with environment A," and ordinations have been criticized for lack of interpretability (47). Below, a framework is introduced that back-transforms an individual's multivariate RDA score into an estimate of the quantitative trait value for that individual. This back-transformation is an extension of RDA for predicting environmental traits from landscape genomic data (only genotypes and environments) and is biologically interpretable as a standardized trait value. The accuracy of the back-transformation scales with the degree that the phenotype evolves to be correlated with the environmental variable and is unaffected by the false-positive rate of RDA as an outlier method for detecting single nucleotide polymorphisms.

Back-transformation for standardized trait value. The RDA-predicted environmental trait value of individual i in environment j, $\hat{v}_{ij}$, is back-transformed from their score in multivariate space as

$$\hat{v}_{ij} = \sum_{k=1}^{k=c} F_{ik} \lambda_k r_{jk}, \qquad [1]$$

where $\hat{v}_{ij}$ is the RDA-predicted unstandardized environmental trait value, k is the canonical axis, c is the number of canonical axes included in the calculation, F_{ik} is the "site score" of individual i on canonical axis k, λ_k is the eigenvalue of axis k, and r_{jk} is the correlation between environment j and axis k (notation following ref. 48 pp. 579 to 593, see *SI Appendix,* Fig. S14 for conceptual visualization). The unstandardized $\hat{v}_{ij}$ was then converted to a standardized *z*-score for the RDA-predicted trait value. The prediction was calculated from an RDA based on 20,000 loci randomly chosen from the genome. Accuracy of the prediction was calculated as Kendall's correlation between $\hat{v}_{ij}$ and the ground-truth trait value z_{ij} (of individual i in quantitative trait j that adapted to environment j).

Accuracy of back-transformation without structure correction. For the basic RDA model without structure correction, across all simulations there was a positive correlation between the RDA-predicted environmental trait for each individual (predicted from its scores in RDA space, Eq. **1**) and the ground-truth evolved value (Fig. 5*C*). Accuracy was not affected by the genic level of the architecture (Fig. 5*C* and *SI Appendix,* Fig. S15). Surprisingly, the prediction was accurate even when unique combinations of QTNs resulted in similar trait values (*SI Appendix,* Fig. S16). The accuracy of the RDA-predicted trait value was determined primarily by the degree that the trait evolved to be correlated with the environment (*SI Appendix,* Fig. S17) and secondarily by the demography (*SI Appendix,* Table S3). Note, however, that
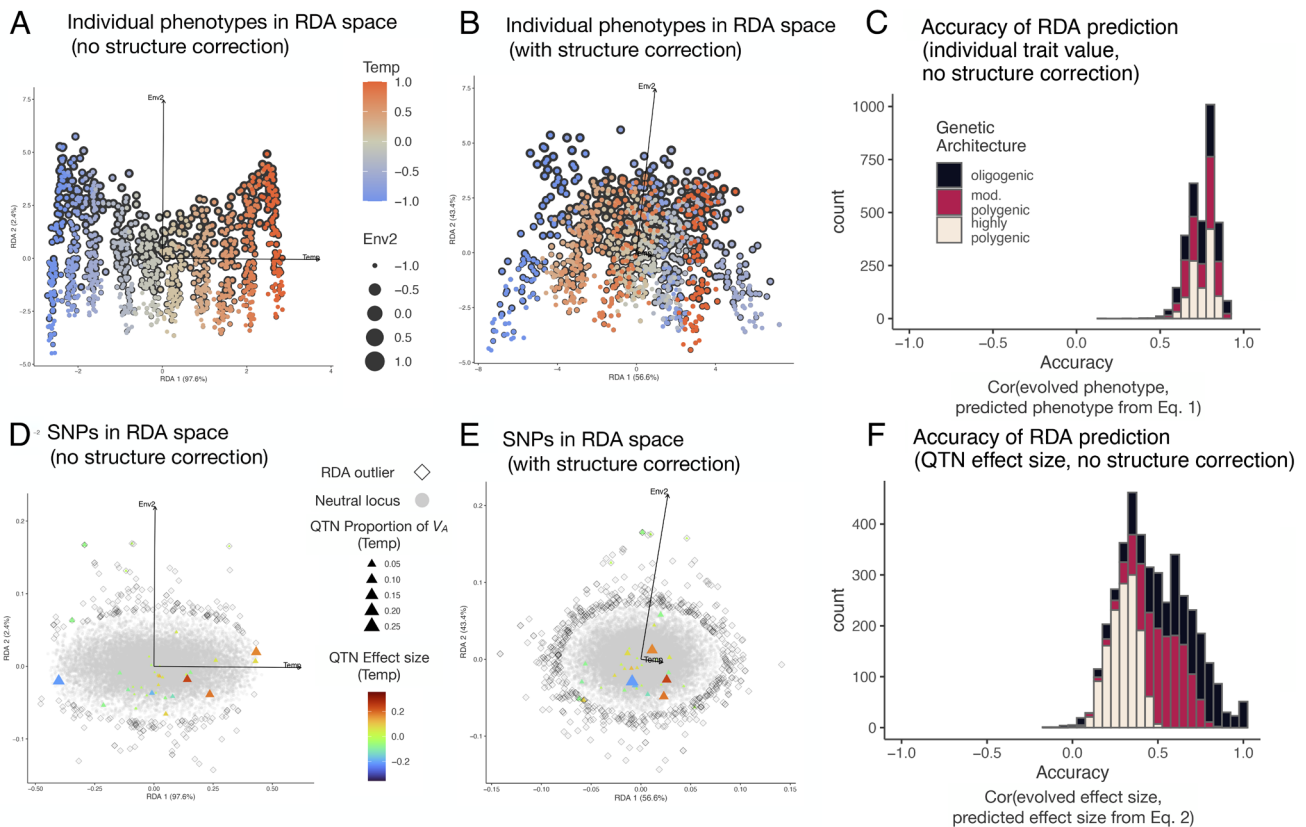
Fig. 5. Evaluation of redundancy analysis (RDA) model with genotype as a function of the environment. (*A*) RDA plots with individuals colored according to their evolved multivariate trait value without a correction for structure or (*B*) in a pRDA with a structure correction. (*C*) Across both traits, accuracy of the RDA-predicted individual trait value from Eq. **1** based on that individual's score in RDA space. Accuracy was measured as the correlation between the evolved trait value and the RDA prediction. (*D*) RDA plots with single-nucleotide polymorphisms (SNPs) colored according to their effect on the temperature trait without a correction for structure or (*E*) in a pRDA with a structure correction. QTNs are colored according to their effect size on the trait and the point size corresponds to the proportion of additive genetic variance (V_A). RDA outliers are outlined in black diamonds. (*F*) Accuracy of the RDA-predicted mutation effect size from Eq. **2** based on that QTN's score in RDA space. Accuracy was measured as the correlation between the evolved effect size and the RDA prediction. Parameter levels for *A–E*: Estuary clines landscape, moderately polygenic, two traits with pleiotropy and equal selection strength, *N* central cline, *m* constant, seed 1231214.

the proportion variance explained by each RDA axis did not necessarily reflect how "important" that axis was. For example, due to the higher gene flow for the Env2 trait in Fig. 5*A*, the first RDA axis (on which temperature loaded) explained almost all the variation, even though temperature and *Env2* were weighted equally in the fitness calculation.

Back-transformation for standardized allele effect size. The RDA trait-prediction was accurate even when unique architectures resulted in the same trait value (e.g., *SI Appendix*, Fig. S16), when geographic location was not correlated with trait values (as in *SS-Mtn*), and when the QTNs were not outliers in RDA space. This could occur if the underlying QTN mutations mapped onto RDA space according to their effect size, and traits were a sum of effects of the QTN alleles within each individual genome (Fig. 5*D* for temperature, *SI Appendix*, Fig. S18 for *Env2*). To quantify how accurately QTNs loaded onto RDA axes based on their multivariate effect size, I used a back-transformation framework analogous to Eq. **1**, but for allele effect sizes. The RDA-predicted relative effect size of locus *l* on quantitative trait *j* is

$$\widehat{u}_{ij} = \sum_{k=1}^{k=c} U_{lk} \lambda_k r_{jk}, \qquad [2]$$

where *k* is the canonical axis, *c* is the total number of canonical axes (two in all simulations), U_{lk} is the normalized eigenvector ("species score") for locus *l* on canonical axis *k*, λ_k is the eigenvalue of axis *k*, and r_{jk} is the correlation between environment *j* and

axis *k* (*SI Appendix*, Fig. S14*B*). The unstandardized $\widehat{u}_{ij}$ was then converted to a standardized *z*-score for the RDA-predicted mutation effect size, and accuracy was calculated as Kendall's correlation coefficient between the prediction and the evolved additive effect on the derived allele at that locus on the quantitative trait (ground truth).

The accuracy of Eq. **2** was not affected by pleiotropic effects of single alleles, but accuracy decreased as the genic level increased, due to decreasing allelic effect sizes (Fig. 5*F*). This led to an interesting paradox, because the accuracy of Eq. **1** was not affected by genic level (Fig. 5*C*). The apparent paradox resulted from a balance between two sources of uncertainty in the trait prediction: i) estimation error in the effect size of QTN within the RDA (higher error in polygenic traits with small effects and lower error in oligogenic with large effects) and ii) sampling error that arose from selecting a subset of markers from the simulation to calculate the trait prediction (lower error in polygenic with many loci and higher error in oligogenic with few loci) (*SI Appendix, Supplemental Results: Accuracy of RDA Trait and Mutation Predictions*).

Accuracy of back-transformation with structure correction. Structure correction jumbled the mapping of individuals and mutations in multivariate space (compare Fig. 5*B* with Fig. 5*C* for traits, Fig. 5*E* to Fig. 5*D* for temperature QTNs, and *SI Appendix*, Fig. S18 *A* and *B* for Env2 QTNs). The jumbling primarily occurred along the temperature-loaded RDA axis, which was more correlated with structure. As a result, the pRDA model with structure correction typically had decreased performance for the multivariate trait prediction

Eq. **1** and mutation effect size prediction Eq. **2** (*SI Appendix*, Figs. S18 *C* and *D* and S19).

An accurate prediction of a quantitative trait for an individual from landscape genetic data for a locally adapted species could have potentially useful applications, particularly for traits such as temperature tolerance that can be hard to measure in a standardized way (49). This raised the question of how few markers would be necessary to make an accurate prediction of the trait value. Across a wide range of scenarios, accuracy of the RDA trait-prediction was similar for 5,000 (~15 to 20% of the simulated genome) randomly sampled loci from the genome as it was for 20,000 loci (~60 to 70% of simulated genome), although error was higher in the oligogenic case due to smaller chance of the region of the genome affected by selection being included (*SI Appendix*, Fig. S20).

A Complex Multivariate Case. To explore whether the results were valid in a more complex context, I created a non-Wright–Fisher multivariate range expansion simulation with six moderately polygenic environmental traits, each with spatially heterogeneous trait optima given by a Bioclim environment in western Canada (Fig. 6*A*, simulations extended from 50). The selective Bioclim environments were weakly correlated (*SI Appendix*, Fig. S21). The simulations allowed for pleiotropic effects on any number of traits, with complex correlation patterns evolving among the allele effects on traits (*SI Appendix*, Fig. S22). The parameters resulted in population expansion from three refugia (after burn-in) with allele surfing and secondary contact (Movie S1), which gave rise to complex patterns of admixture and population structure (Fig. 6*C* and *SI Appendix*, Figs. S23 and S24). All six traits evolved local adaptation, as evidenced by high correlations (>0.9) between trait values and environments. The QTNs evolved a mix of clinal and nonmonotonic patterns in allele frequencies across environmental gradients, with 0 to 11% of QTNs showing significant clines (Fig. 6*B*).

The RDA-predicted trait value (estimated from Eq. **1** using the first three redundancy axes) was 60 to 80% accurate, and accuracy was not affected by the addition of three nuisance Bioclim variables in the RDA model (Fig. 6*D* and *SI Appendix*, Fig. S21). Although the trait value of an individual could not always be determined visually from its mapping in an RDA biplot (*SI Appendix*, Fig. S25), the prediction was accurate across environmental variables, regardless of the degree they were correlated with geography or population structure (*SI Appendix*, Fig. S26).
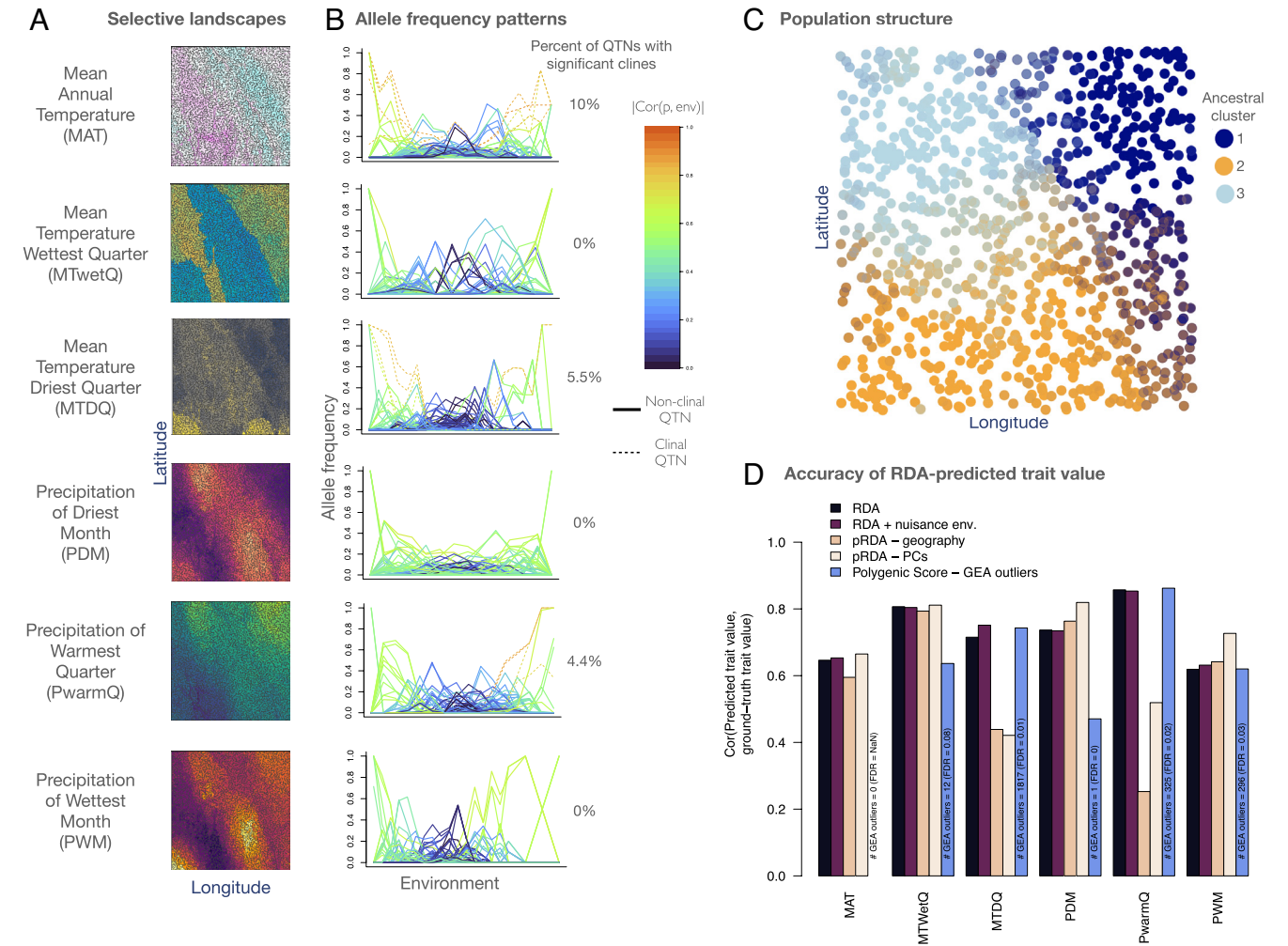

Fig. 6. A complex multivariate case with range expansion and multiple refugia. (*A*) The six selective landscapes from Bioclim in western Canada; background colors correspond to the optimum trait value on each landscape and point colors correspond to the evolved trait value at that location. (*B*) Allele frequency patterns at the derived allele of QTNs for each landscape. (*C*) Evolved population structure on the landscape with individuals colored according to assignment to ancestral clusters. Intermediate colors represent admixture. (*D*) Accuracy of the redundancy analysis (RDA) predicted standardized trait value from Eq. **1** compared among i) the base model, ii) the base model plus the addition of three nuisance Bioclim variables, a pRDA with structure either corrected by iii) geography or iv) principal components, and v) a polygenic score based on genotype–environment associate (GEA) outliers calculated with latent factor mixed models. For the polygenic score, the number of GEA outliers and the false discovery rate (FDR) are shown within the bar for each environment.

Correction for structure only decreased accuracy for the traits that were correlated with the first two principal components of population structure, or both latitude and longitude, with little effect on the accuracy for other traits (Fig. 6*D* and *SI Appendix,* Fig. S26). The RDA-predicted trait value Eq. **1** was as accurate or more accurate than a polygenic score based on GEA outliers from univariate latent factor mixed models (Fig. 6*D*). Indeed, for mean annual temperature, a polygenic score could not be predicted because there were no outliers (Fig. 6*D*).

Applications of redundancy analysis in the Literature. Current applications of RDA in the literature fall into two categories i) use as an outlier method to detect the genetic basis of environmental adaptation (which this study shows has high false-positive rates), and ii) as a visualization tool to understand how populations/ genotypes are correlated with environments (which this study shows can be an accurate approximation for an quantitative trait). I surveyed the literature for peer-reviewed papers that cited (32) and were published since 2021. Of the 10 studies that met those criteria, 90% of them used RDA to detect outliers, while 40% used RDA to visualize how populations are correlated with environments (*SI Appendix,* Table S4). Thus, the proportion of studies that currently use RDA for outlier detection, which this study shows is plagued by false positives, is roughly twice as high as those that use it for understanding population-level adaptation. Additionally, 40% of the studies included a structure correction in the RDA, which this research shows can affect the accuracy of inference (*SI Appendix,* Table S4).

Discussion

Population genetic models of adaptation to a heterogeneous environment that assume selection acts directly on the locus predict that frequency clines will evolve at alleles under selection (2, 5–8). Much of the existing literature on polygenic adaptation has focused on whether subtle allele frequency changes along environmental gradients result in detectable clines, which is a concept that falls under the GEA paradigm (16, 51). Given this body of literature, the evolution of adaptive trait clines with nonmonotonic patterns in the underlying allele frequencies initially seems like a paradox. The paradox arises through a quantitative genetic model of selection, under conditions that promote unique combinations of mutations to evolve to the multivariate optimum in different parts of the landscape.

By adding spatial complexity, this research demonstrates how genotypic redundancy [i.e., multiple possible genotypes that lead to a similar phenotype; (43)] can interact with pleiotropy and reduced gene flow (42) to evolve to nonmonotonic patterns between allele frequencies at quantitative-trait nucleotides and each environmental variable. In this case, trait adaptation proceeds via unique allelic combinations in different demes, which can lead to unexpected patterns at the underlying alleles (51, 52). These unique allelic combinations are analogous to modular genetic architectures, which have been predicted to evolve in complex environments (47, 53–55).

Such complex possibilities were verbally predicted by Barton in 1979 (8), but have not been elucidated until now. This research also demonstrates, however, that genotypic redundancy is not required to evolve nonlinearities. Oligogenic architectures with low redundancy evolved nonclinal patterns when pleiotropic effects allowed unique combinations of mutations to achieve a spatially varying multivariate optimum. Although this study focused on environmental gradients across space, similarly unexpected patterns could evolve in response to environmental change through time.

Recent reviews have concluded that polygenic architectures are common in environmental adaptation (11, 56) and that pleiotropy is common in adaptive divergence (57), indicating that the paradox could be common. The simulations raise interesting questions that could be tested empirically, such as i) what kind of patterns between allele frequency and environment evolve at hits for adapted traits in genome-wide association studies?; ii) what proportion of additive genetic variance is explained by clinal alleles?; iii) what proportion of total local adaptation can be explained by clinal alleles?; and iv) how well does multivariate trait prediction from landscape genomic data predict empirically measured multivariate traits? This research also raises questions about the extent to which local adaptation is nonparallel on different kinds of landscapes (e.g., stepping stone vs. estuary), which can now be quantified by estimating evolutionary constraint (58).

In addition, this research can explain why clines in allele frequencies at genes that underlie environmental traits do not always evolve. For example, using quantitative trait loci underlying traits that had clines with environmental gradients, Mahoney et al. discovered some sets of loci that showed nonclinal patterns of increasing and decreasing allele frequencies across an environmental gradient as predicted by this study (59). More empirical studies applying the frameworks proposed here are needed to determine the importance of clinal alleles in adaptation. If such nonmonotonic patterns are common in nature, these results raise questions about the utility of current GEA methods for accurately inferring the genetic architecture of adaptation to complex environments. The challenges with GEAs are not only the question of whether allele frequency clines have evolved in the system, but also how to know in any particular system the extent to which inference is plagued by false positives and false negatives, and how to correct for structure.

With regard to the question of whether the utility of GEA methods should be reassessed, it depends on the study question. If the study question seeks to accurately infer the genetic basis of adaptation to the environment, GEA methods will be limited primarily by first principles (the number of quantitative-trait nucleotides that evolve clines) and secondarily by statistical issues associated with correction for population structure (either riddled with false positives without structure correction, or decreased power with structure correction if structure correlates with the selective environment). This latter "catch-22" raises the possibility that GEA methods will only accurately infer QTNs within a limited parameter space.

On the other hand, if the study question seeks to predict something about local adaptation in the population, in some systems a few true-positive clinal QTNs that explain broad-scale geographic patterns of adaptation may be sufficient for the prediction. Various methods for genomic forecasting and genomic offset have been proposed to meet the challenges of biodiversity management under climate change, but many of them incorporate GEA methods (60–62). Such gene-targeted conservation approaches have been criticized because of the difficulty in knowing whether the genomic basis of adaptation has been accurately inferred (63–65). Results from this study suggest that GEA results may be sufficient to forecast broad-scale biogeographic patterns in some systems but not others.

Despite the limitations of GEA methods, this study highlights how multivariate trait prediction can be accurate without knowledge of the genetic architecture. Interestingly, the RDA trait prediction (Eq. **1**) was accurate even when two individuals had different genetic architectures that gave the same trait value, when QTNs were not outliers in RDA space, when geographic location was not correlated with trait values, and for environmental

variables that were not correlated with population structure. This occurred because prior to ordination in the RDA, each locus is used in a multiple regression model with the environmental variables to produce fitted values for that locus across individuals. Thus, there is flexibility with the RDA to capture the way environmental variables may influence the patterns at one locus in a different way than at another locus, which may not correlate with the relationship between the environment and population structure (Supplemental Tutorial). Additionally, the multivariate trait prediction was more accurate without a correction for structure in the RDA, because structure correction jumbled the multivariate mapping of loci and individuals along the environment(s) that were more correlated with structure.

The results herein highlight that using ordination or other genomic prediction methods to predict multivariate trait values at the level of the individual could prove more fruitful across a wide range of scenarios than identifying GEA outliers. These prediction methods require that linked loci are included in the data (66). Whether such trait predictions from genomic and environmental data will be accurate with dominance, epistatic interactions, trait plasticity, and/or with nonlinear relationships between the trait optimum and environmental variable remains an important direction for future research. An important next step for empirical research will be to validate the RDA trait prediction by comparing it with ground-truth trait values obtained through experimental measures of traits in common garden environments. Biodiversity management in the face of rapid, multivariate climate change in the world's terrestrial and marine systems remains an urgent societal need (67, 68). If multivariate trait predictions meet an acceptable level of performance through this validation process (reviewed in ref. 69), these predictions could prove useful for genomic forecasting, as well as choosing individuals for restoration or assisted gene flow efforts.

Materials and Methods

Landscapes and Demographies. All simulations consisted of 100 demes arranged on a 10 × 10 landscape grid (Fig. 1*A*). The 15 levels of landscape-demography were broadly divided into three landscape categories (Fig. 1*A*): i) a stepping stone landscape with latitudinal and longitudinal selective clines (Stepping-Stone Clines, the most commonly simulated scenario in testing methods) (14, 20, 22–24, 27–30), ii) a stepping stone landscape with one latitudinal cline and one nonlinear longitudinal mountain range (Stepping-Stone Mountain, which left the potential for unique architectures to arise to the same selective pressure at different geographic locations), and iii) an estuary landscape with a latitudinal and longitudinal selective clines (Estuary Clines, which simulated repeated independent bouts of adaptation analogous to oysters or sticklebacks that repeatedly colonize and adapt to isolated freshwater environments connected by gene flow in the marine environment). For simplicity, I refer to the latitudinal environment as Temperature and the longitudinal environment as *Env2*.

In summary, Stepping-Stone Mountain had a different environmental pattern than Stepping-Stone Clines but the same demography, while Estuary Clines had the same environmental pattern as Stepping-Stone Clines but different demography (Fig. 1*A*). The demographic parameters were chosen such that different landscapes achieved similar levels of neutral genetic differentiation and local adaptation. Within each of the three landscapes, five demographies were simulated that described the migration rates and effective population sizes on the landscape (Fig. 1*B* and *SI Appendix, Supplemental Methods* and Figs. S27 and S28 and Tables S5 and S6).

See *SI Appendix, Supplemental Methods* for a description of the multivariate continuous space simulations with six traits.

Genetic Map. The Wright–Fisher simulations were based on a previously published quantitative genetic model and a genetic map (50). The genome consisted of 20 linkage groups each with 50,000 sites. The scaled recombination rate ($N_{metapop} r = 0.01$) gave a resolution of 0.001 cM between proximate bases

and a total length of 50 cM for each linkage group. This resolution mimicked a single-nucleotide polymorphism chip, in which loci were collected across a large genetic map (50). The population-scaled neutral mutation rate was ($N_{metapop} \mu = 0.001$). QTNs could evolve on the first 10 linkage groups, while on the second 10 linkage groups, only neutral loci could evolve.

Genetic Architecture and Stabilizing Selection.

Mutation. Quantitative trait nucleotides contributed additively to the optimal phenotype for each individual without dominance. Three genic levels were simulated: oligogenic (few loci of large effect on the trait), moderately polygenic (dozens to hundreds of loci with intermediate effects), and highly polygenic (hundreds of loci with small effects Fig. 1*C* and *SI Appendix*, Table S7). For QTN mutations under one trait or two traits without pleiotropy, the univariate effect size of a QTN mutation was drawn from a normal distribution with a mean of 0 and SD σ_{QTN} (*SI Appendix*, Table S7). For QTN mutations under two traits with pleiotropy, the bivariate effect size was drawn from a multivariate normal distribution with a SD of σ_{QTN} for both traits and no covariance, which gave flexibility for mutations to evolve with effects on one or both traits. Thus, the distribution of effect sizes and linkage relationships among QTNs was allowed to evolve.

Pleiotropy. Within each genic category were five levels of pleiotropy and selection: i) one temperature trait (which adapted to the latitudinal cline), ii) two traits without pleiotropy and equal strengths of selection on both traits, iii) two traits without pleiotropy and with weaker selection on the temperature trait, iv) two traits with pleiotropy (QTNs could evolve effects on one or both traits) and equal strengths of selection on both traits, and v) two traits with pleiotropy and with weaker selection on the latitudinal temperature trait (Fig. 1*D* and *SI Appendix*, Table S8).

Selection. The trait was subject to spatially heterogeneous stabilizing selection with the optimum for each location in space given by the environment. For each individual in each generation, the fitness was determined by a Gaussian function given the difference between the individual's phenotype and the optimum at that location. For two traits, the fitness for individual *i* at location *{x,y}* was

$$\omega_{ixy} = 1 - \frac{\exp\left(-\frac{1}{2}\left(\mathbf{X}_i - \Theta_{xy}\right)^T \Sigma^{-1}\left(\mathbf{X}_i - \Theta_{xy}\right)\right)}{\sqrt{(2\pi)^k |\Sigma|}}, \quad [3]$$

where $\mathbf{X}_i$ is a vector of phenotypic values for individual *i* in deme *xy* and Θ_{xy} is a vector of phenotypic optimums for that deme (optimums shown in Fig. 1*A*). Σ is the symmetric variance-covariance matrix representing the strength of selection on each trait within a deme. For two traits, Σ is a 2 × 2 matrix with the strength of selection on the diagonals (Fig. 1*D* and *SI Appendix*, Table S8) and zero covariance. For one trait, this equation reduces to the normal distribution.

For information on burnin, adding neutral loci with tree sequencing, filtering, and sampling, see *SI Appendix, Supplemental Methods*.

Quantifying the Degree of Local Adaptation, Divergence, and Structure. For each replicate, the degree of local adaptation was measured as i) the difference between population fitness in sympatry and allopatry following (46) and ii) the correlation between the phenotype and environmental cline for each trait. Overall divergence (genetic differentiation) was calculated as Weir and Cockerham's F_{ST} (70) in OutFLANK (71). Population structure was estimated with a principal component analysis on the genotype matrix.

Quantifying Trait and Allelic Clines. The degree of a trait cline was measured as Kendall's τ rank correlation coefficient between individual trait values and deme environment. The degree of an allele frequency cline was measured as Kendall's τ rank correlation coefficient (72, 73) between deme allele frequency and deme environment, with significance being determined after Bonferroni correction based on the number of single nucleotide polymorphisms in the data. QTNs that were significant by this criteria were deemed clinal QTNs. The proportion of clinal QTNs excluded minor alleles with frequency < 0.01.

GEA Performance. Latent-factor mixed models assess the linear relationship between genotype and environment while controlling for structure as latent factors. Latent factor mixed models was implemented using the function lfmm2 in the R package LEA v.4.0.3 (20, 21, 25). Redundancy analysis (RDA) and the partial RDA (pRDA) including a structure correction (conditional on the first two PC axes) were implemented using the 'rda' function in the R package vegan

(74). See *SI Appendix, Supplemental Methods* for details of implementation and correction for false discovery rate.

The performance of the association metrics was summarized as i) false discovery rate (FDR, proportion of outliers that are neutral, lower is better), ii) true-positive rate (TPR, proportion of QTNs that are significant outliers, higher is better), and iii) the area under the precision-recall curve (higher is better) (69). In order to provide the most optimistic estimate of a method's performance, the performance statistics were calculated by only including truly neutral loci unaffected by selection on linkage groups 11 to 20 and the QTNs.

Importance of Clinal QTNs to Local Adaptation.

First framework. A linear model was used to conduct the genome-wide association study with individual trait value as the response variable and genotype, PC1, and PC2 as explanatory variables. The proportion of genome-wide association hits that also showed clines with the environmental variable was compared with the known number of clinal QTNs.

Second framework. The proportion of additive genetic variance (V_A) for each QTN was calculated as the additive genetic variance for the focal QTN standardized by the total additive genetic variance following (50). The proportion of additive genetic variance (V_A) explained by clinal QTNs was compared with a null expectation equal to the proportion of QTNs that were clinal.

Third framework. The proportion of local explained was estimated for different subsets of QTNs: i) QTNs with minor allele frequency > 0.01, ii) clinal QTNs, and iii) clinal QTNs inferred from latent factor mixed models that include a structure correction. For ii) and iii), a GEA model was performed for each environment, and then outlier QTNs were combined into a focal QTN set that was used for the local adaptation prediction. For each focal subset of QTNs, the counts of the derived allele were multiplied by the QTN effect size, summed to get a phenotype, and that phenotype was used in an in silico reciprocal transplant using the known phenotype-fitness function to estimate the degree of local adaptation. This estimate was then divided by the total degree of local adaptation (using all QTNs including those below the minor allele frequency threshold) to get an estimate of the proportion of local adaptation explained by that focal subset.

Data, Materials, and Software Availability. A Supplemental Tutorial that shows how to implement Eq. **1** in R and demonstrates other properties of redundancy analysis is published on the MarineOmics page at https://marineomics.github.io/RDAtraitPredictionTutorial.html (75). The code used to produce all the simulations and results is archived at https://doi.org/10.5281/zenodo.7622893 (76). Simulation output files are archived at https://www.bco-dmo.org/dataset/889769 (77).

1. J. Huxley, Clines: An auxiliary taxonomic principle. *Nature* **142**, 219–220 (1938).
2. J. A. Endler, Geographic variation, speciation, and clines. *Monogr. Popul. Biol.* **10**, 1–246 (1977).
3. J. B. S. Haldane, The theory of a cline. *J. Genet.* **48**, 277–284 (1948).
4. P. Holgate, Genotype frequencies in a section of a cline. *Heredity* **19**, 507–509 (1964).
5. R. M. May, J. A. Endler, R. E. McMurtrie, Gene frequency clines in the presence of selection opposed by gene flow. *Am. Nat.* **109**, 659–676 (1975).
6. J. A. Endler, Gene flow and population differentiation. *Science* **179**, 243–250 (1973).
7. R. A. Fisher, Gene frequencies in a cline determined by selection and diffusion. *Biometrics* **6**, 353–361 (1950), 10.2307/3001780.
8. N. H. Barton, Gene flow past a cline. *Heredity* **43**, 333–339 (1979).
9. A. M. Westram, K. Faria, K. Johannesson, R. Butlin, N. Barton, Inversions and parallel evolution. *Philos. Trans. R. Soc. Lond. B Biol. Sci.* **377**, 20210203 (2022).
10. N. H. Barton, Clines in polygenic traits. *Genet. Res.* **74**, 223–236 (1999).
11. O. Savolainen, M. Lascoux, J. Merilä, Ecological genomics of local adaptation. *Nat. Rev. Genet.* **14**, 807–820 (2013).
12. T. Dobzhansky, R. C. Lewontin, *Dobzhansky's Genetics of Natural Populations I-XLIII* (Columbia University Press, 2003).
13. P. W. Hedrick, Genetic polymorphism in heterogeneous environments: The age of Genomics. *Annu. Rev. Ecol. Evol. Syst.* **37**, 67–93 (2006).
14. C. Rellstab, F. Gugerli, A. J. Eckert, A. M. Hancock, R. Holderegger, A practical guide to environmental association analysis in landscape genomics. *Mol. Ecol.* **24**, 4348–4370 (2015).
15. S. Hoban *et al.*, Finding the genomic basis of local adaptation: Pitfalls, practical solutions, and future directions. *Am. Nat.* **188**, 379–397 (2016).
16. J. K. Pritchard, J. K. Pickrell, G. Coop, The genetics of human adaptation: Hard sweeps, soft sweeps, and polygenic adaptation. *Curr. Biol.* **20**, R208–R215 (2010), 10.1016/j.cub.2009.11.055.
17. A. M. Hancock, G. Alkorta-Aranburu, D. B. Witonsky, A. Di Rienzo, Adaptations to new environments in humans: The role of subtle allele frequency shifts. *Philos. Trans. R. Soc. Lond. B Biol. Sci.* **365**, 2459–2468 (2010).
18. M. Fumagalli *et al.*, Signatures of environmental genetic adaptation pinpoint pathogens as the main selective pressure through human evolution. *PLoS Genet.* **7**, e1002355 (2011).
19. A.-M. Waldvogel, D. Schreiber, M. Pfenninger, B. Feldmeyer, Climate change genomics calls for standardized data reporting. *Front. Ecol. Evol.* **8** (2020), https://doi.org/10.3389/fevo.2020.00242.
20. E. Frichot, S. D. Schoville, G. Bouchard, O. François, Testing for associations between loci and environmental gradients using latent factor mixed models. *Mol. Biol. Evol.* **30**, 1687–1699 (2013).
21. E. Frichot, O. François, LEA: An R package for landscape and ecological association studies. *Methods Ecol. Evol.* **6**, 925–929 (2015).
22. P. L. Ralph, G. Coop, Robust identification of local adaptation from allele frequencies. *Genetics* **195**, 205–220 (2013).
23. M. Gautier, Genome-wide scan for adaptive divergence and association with population-specific covariates. *Genetics* **201**, 1555–1579 (2015).
24. G. Coop, D. Witonsky, A. Di Rienzo, J. K. Pritchard, Using environmental correlations to identify loci underlying local adaptation. *Genetics* **185**, 1411–1423 (2010).
25. K. Caye, B. Jumentier, J. Lepeule, O. François, LFMM 2: Fast and accurate inference of gene-environment associations in genome-wide studies. *Mol. Biol. Evol.* **36**, 852–860 (2019).
26. C. W. Ahrens *et al.*, The search for loci under selection: Trends, biases and progress. *Mol. Ecol.* **27**, 1342–1356 (2018).
27. K. E. Lotterhos, M. C. Whitlock, The relative power of genome scans to detect local adaptation depends on sampling design and statistical method. *Mol. Ecol.* **24**, 1031–1046 (2015).
28. P. de Villemereuil, É. Frichot, É. Bazin, O. François, O. E. Gaggiotti, Genome scan methods against more complex models: When and how much should we trust them? *Mol. Ecol.* **23**, 2006–2019 (2014).
29. B. R. Forester, J. R. Lasky, H. H. Wagner, D. L. Urban, Comparing methods for detecting multilocus adaptation with multivariate genotype-environment associations. *Mol. Ecol.* **27**, 2215–2233 (2018).
30. B. R. Forester, M. R. Jones, S. Joost, E. L. Landguth, J. R. Lasky, Detecting spatial genetic signatures of local adaptation in heterogeneous landscapes. *Mol. Ecol.* **25**, 104–120 (2016).
31. T. Capblancq, K. Luu, M. G. B. Blum, E. Bazin, Evaluation of redundancy analysis to identify signatures of local adaptation. *Mol. Ecol. Resour.* **18**, 1223–1233 (2018).
32. T. Capblancq, B. R. Forester, Redundancy analysis: A swiss army knife for landscape genomics. *Methods Ecol. Evol.* **12**, 2298–2309 (2021).
33. A. M. Hancock *et al.*, Adaptations to climate-mediated selective pressures in humans. *PLoS Genet.* **7**, e1001375 (2011).
34. L. M. Evans *et al.*, Population genomics of *Populus trichocarpa* identifies signatures of selection and adaptive trait associations. *Nat. Genet.* **46**, 1089–1096 (2014).
35. S. Yeaman *et al.*, Convergent local adaptation to climate in distantly related conifers. *Science* **353**, 1431–1433 (2016).
36. J. Russell *et al.*, Exome sequencing of geographically diverse barley landraces and wild relatives gives insights into environmental adaptation. *Nat. Genet.* **48**, 1024–1030 (2016).
37. P. R. Berg *et al.*, Adaptation to low salinity promotes genomic divergence in Atlantic Cod (*Gadus morhua* L.). *Genome Biol. Evol.* **7**, 1644–1663 (2015).
38. T. S. Kuhn, *The Structure of Scientific Revolutions: 50th* (University of Chicago Press, ed. Anniversary, 2012).
39. T. S. Kuhn, *The Essential Tension: Selected Studies in Scientific Tradition and Change* (University of Chicago Press, 1979).
40. B. C. Haller, P. W. Messer, SLiM 3: Forward genetic simulations beyond the Wright-Fisher model. *Mol. Biol. Evol.* **36**, 632–637 (2019).
41. B. C. Haller, J. Galloway, J. Kelleher, P. W. Messer, P. L. Ralph, Tree-sequence recording in SLiM opens new horizons for forward-time simulation of whole genomes. *Mol. Ecol. Resour.* **19**, 552–566 (2019).
42. P. L. Ralph, G. Coop, Convergent evolution during local adaptation to patchy landscapes. *PLoS Genet.* **11**, e1005630 (2015).
43. Á. J. Láruson, S. Yeaman, K. E. Lotterhos, The importance of genetic redundancy in evolution. *Trends Ecol. Evol.* **35**, 809–822 (2020).
44. J. R. Lasky *et al.*, Characterizing genomic variation of *Arabidopsis thaliana*: The roles of geography and climate. *Mol. Ecol.* **21**, 5512–5529 (2012).
45. M. Lynch, B. Walsh, *Genetics and Analysis of Quantitative Traits* (Oxford University Press, 1998). http://www.invemar.org.co/redcostera1/invemar/docs/RinconLiterario/2011/febrero/AG_8.pdf.
46. F. Blanquart, O. Kaltz, S. L. Nuismer, S. Gandon, A practical guide to measuring local adaptation. *Ecol. Lett.* **16**, 1195–1205 (2013).
47. K. E. Lotterhos, S. Yeaman, J. Degner, S. Aitken, K. A. Hodgins, Modularity of genes involved in local adaptation to climate despite physical linkage. *Genome Biol.* **19**, 157 (2018).
48. P. Legendre, L. Legendre, *Numerical Ecology* (Elsevier, Amsterdam, The Netherlands, 1998).
49. J. C. Havird *et al.*, Distinguishing between active plasticity due to thermal acclimation and passive plasticity due to Q 10 effects: Why methodology matters. *Funct. Ecol.* **34**, 1015–1028 (2020).
50. K. E. Lotterhos, The effect of neutral recombination variation on genome scans for selection. *G3 (Bethesda)* **9**, 1851–1867 (2019).
51. S. Yeaman, Local adaptation by alleles of small effect. *Am. Nat.* **186**, S74–S89 (2015).
52. V. Le Corre, A. Kremer, The genetic differentiation at quantitative trait loci under local adaptation. *Mol. Ecol.* **21**, 1548–1566 (2012).
53. G. P. Wagner, Homologues, natural kinds and the evolution of modularity. *Integr. Comp. Biol.* **36**, 36–43 (1996).
54. C. K. Griswold, Pleiotropic mutation, modularity and evolvability. *Evol. Dev.* **8**, 81–93 (2006).
55. H. Le Nagard, L. Chao, O. Tenaillon, The emergence of complexity and restricted pleiotropy in adapting networks. *BMC Evol. Biol.* **11**, 326 (2011).
56. B. M. Lind, M. Menon, C. E. Bolte, T. M. Faske, A. J. Eckert, The genomics of local adaptation in trees: Are we out of the woods yet? *Tree Genet. Genomes* **14**, 29 (2018).

57. K. A. Thompson, Experimental hybridization studies suggest that pleiotropic alleles commonly underlie adaptive divergence between natural populations. *Am. Nat.* **196**, E16–E22 (2020).

58. S. Yeaman, A. C. Gerstein, K. A. Hodgins, M. C. Whitlock, Quantifying how constraints limit the diversity of viable routes to adaptation. *PLoS Genet.* **14**, e1007717 (2018).

59. C. R. Mahony *et al.*, Evaluating genomic data for management of local adaptation in a changing climate: A lodgepole pine case study. *Evol. Appl.* **13**, 116–131 (2020).

60. C. Rellstab, B. Dauphin, M. Exposito-Alonso, Prospects and limitations of genomic offset in conservation management. *Evol. Appl.* **14**, 1202–1212 (2021).

61. Á. J. Láruson, M. C. Fitzpatrick, S. R. Keller, B. C. Haller, K. E. Lotterhos, Seeing the forest for the trees: Assessing genetic offset predictions from gradient forest. *Evol. Appl.* **15**, 403–416 (2022).

62. A.-M. Waldvogel *et al.*, Evolutionary genomics can improve prediction of species' responses to climate change. *Evol Lett* **4**, 4–18 (2020).

63. M. Kardos, A. B. A. Shafer, The peril of gene-targeted conservation. *Trends Ecol. Evol.* **33**, 827–839 (2018).

64. M. A. Russello, S. L. Kirk, K. K. Frazer, P. J. Askey, Detection of outlier loci and their utility for fisheries management. *Evol. Appl.* **5**, 39–52 (2012).

65. S. P. Flanagan, B. R. Forester, E. K. Latch, S. N. Aitken, S. Hoban, Guidelines for planning genomic assessment and monitoring of locally adaptive variation to inform species conservation. *Evol. Appl.* **11**, 1035–1052 (2018).

66. B. C. Y. Collard, D. J. Mackill, Marker-assisted selection: An approach for precision plant breeding in the twenty-first century. *Philos. Trans. R. Soc. Lond. B Biol. Sci.* **363**, 557–572 (2008).

67. K. E. Lotterhos, Á. J. Láruson, L.-Q. Jiang, Novel and disappearing climates in the global surface ocean from 1800 to 2100. *Sci. Rep.* **11**, 15535 (2021).

68. J. W. Williams, S. T. Jackson, J. E. Kutzbach, Projected distributions of novel and disappearing climates by 2100 AD. *Proc. Natl. Acad. Sci. U. S. A.* **104**, 5738–5742 (2007).

69. K. E. Lotterhos, M. C. Fitzpatrick, H. Blackmon, Simulation tests of methods in evolution, ecology, and systematics: Pitfalls, progress, and principles. *Annu. Rev. Ecol. Evol. Syst.* **53**, 113–136 (2022).

70. B. S. Weir, C. C. Cockerham, Estimating F-statistics for the analysis of population structure. *Evolution* **38**, 1358–1370 (1984).

71. M. C. Whitlock, K. E. Lotterhos, Reliable detection of loci responsible for local adaptation: Inference of a null model through trimming the distribution of F_{ST}. *Am. Nat.* **186**, S24–S36 (2015).

72. M. G. Kendall, A new measure of rank correlation. *Biometrika* **30**, 81–93 (1938).

73. M. G. Kendall, The treatment of ties in ranking problems. *Biometrika* **33**, 239–251 (1945).

74. P. Dixon, VEGAN, a package of R functions for community ecology. *J. Veg. Sci.* **14**, 927–930 (2003).

75. K. E. Lotterhos, RDA trait prediction tutorial. MarineOmics. https://marineomics.github.io/RDAtraitPredictionTutorial.html. Deposited 8 February 2023.

76. K. E. Lotterhos, The paradox of adaptive trait clines with non-clinal patterns in the underlying genes. Zenodo. https://zenodo.org/record/7622893 . Deposited 8 February 2023.

77. K. E. Lotterhos, Dataset: Paradox of adaptive trait clines. Biological and Chemical Oceanography Data Management Office. https://www.bco-dmo.org/dataset/889769. Deposited 13 February 2023.